Journal for ImmunoTherapy of Cancer

T cell-specific non-viral DNA delivery and in vivo CAR-T generation using targeted lipid nanoparticles

Jaime Fernández Bimbo ,[1] Eline van Diest,[1] Daniel E Murphy,[1] Ator Ashoti,[1] Martijn J W Evers,[1] Suneel A Narayanavari,[1] Diana Pereira Vaz,[1] Hanneke Rijssemus,[1] Christina Zotou,[1] Nadine Saber,[2] Zhiyong Lei,[1,2] Peter Mayrhofer,[3,4] Maurits Geerlings,[3,4] Raymond Schiffelers ,[1,2] Jacek Lubelski [1]

To cite: Bimbo JF, van Diest E, Murphy DE, *et al*. T cell-specific non-viral DNA delivery and in vivo CAR-T generation using targeted lipid nanoparticles. *Journal for ImmunoTherapy of Cancer* 2025;**13**:e011759. doi:10.1136/jitc-2025-011759

► Additional supplemental material is published online only. To view, please visit the journal online (https://doi.org/10.1136/jitc-2025-011759).

JFB, EvD and DEM contributed equally.

Accepted 19 June 2025

[1]R&D, NanoCell Therapeutics BV, Utrecht, Utrecht, Netherlands
[2]Central Diagnostisch Laboratorium, University Medical Centre Utrecht, Utrecht, Utrecht, Netherlands
[3]R&D, NanoCell Therapeutics, Wayne, Pennsylvania, USA
[4]Supercoiled GeneTx GmbH, Vienna, Austria

Correspondence to
Dr Jacek Lubelski;
jlubelski@nanocelltx.com

ABSTRACT

Background Ex vivo chimeric antigen receptor (CAR)-T therapies have revolutionized cancer treatment. However, treatment accessibility is hindered by high costs, long manufacturing times, and the need for specialized centers and inpatient care. Strategies to generate CAR-T cells in vivo have emerged as a promising alternative that could bypass CAR-T manufacturing bottlenecks. Most current in vivo CAR-T approaches, while demonstrating encouraging preclinical efficacy, rely on transient messenger RNA (mRNA) delivery or viral vectors which both have limitations in terms of efficiency, durability, and scalability. To address these challenges, we developed a novel DNA-based targeted lipid nanoparticle (LNP) which we termed NCtx.

Methods Minicircle DNA (mcDNA) encoding a CAR construct and SB100x transposase mRNA were encapsulated within a novel lipid formulation which was functionalized with T cell-specific anti-CD7 and anti-CD3 binders. In vitro, we evaluated T cell specificity, mcDNA and mRNA transfection efficiency, transposon-mediated CAR integration and functionality of the resulting CAR-T cells. In vivo efficacy was assessed in peripheral blood mononuclear cell and $CD34^+$ stem cell humanized murine xenograft models of B cell leukemia.

Results In vitro, NCtx displayed high specificity and transfection efficiency with both mcDNA and mRNA in primary T cells. Transposase mRNA facilitated genomic integration of the CAR gene, leading to the generation of stable CAR-T cells that exhibited antigen-specific cytotoxicity and cytokine release. In vivo, a single intravenous dose of NCtx induced robust CAR-T cell generation resulting in effective tumor control and significantly improved survival in two distinct xenograft models.

Conclusions Our findings demonstrate for the first time that targeted LNPs can be employed for efficient DNA delivery to T cells in vitro and in vivo. We show that when combined with transposase technology, this LNP-based system can efficiently generate stable CAR-T cells directly in vivo, inducing potent and durable antitumor responses. NCtx represents a novel non-viral gene therapy vector for in vivo CAR-T therapy, offering a scalable and potentially more accessible alternative to traditional approaches in CAR-T cell generation.

WHAT IS ALREADY KNOWN ON THIS TOPIC

⇒ Ex vivo chimeric antigen receptor (CAR)-T therapies are transformative but remain limited by high costs, complex manufacturing, and restricted patient access. In vivo CAR-T approaches offer a promising alternative but have relied on viral vectors or transient messenger RNA (mRNA) delivery, which still face important challenges in efficiency, durability, and scalability.

WHAT THIS STUDY ADDS

⇒ We developed NCtx, the first lipid nanoparticle-based system capable of delivering DNA to T cells and enabling in vivo CAR-T generation. By encapsulating minicircle DNA and transposase mRNA, NCtx drives genomic CAR integration, resulting in durable CAR-T cells with potent antitumor activity.

HOW THIS STUDY MIGHT AFFECT RESEARCH, PRACTICE, OR POLICY

⇒ This non-viral, scalable, and cost-effective platform provides a novel strategy for in vivo CAR-T therapy, potentially simplifying treatment and broadening patient access. It establishes a foundation for next-generation strategies for in vivo gene engineering of T cells.

INTRODUCTION

Chimeric antigen receptor T cell (CAR-T) therapy has revolutionized the treatment of certain cancers, showing remarkable efficacy in the treatment of hematologic malignancies.[1 2] Conventionally, this therapy relies on an ex vivo manufacturing approach, in which T cells are isolated from the patient and genetically engineered to express CAR before expansion and reinfusion.[3] While this method has proven successful, it is accompanied by significant challenges, including high manufacturing costs, complex logistics and inequality in treatment access.[4 5] Patients often experience delays in therapy due to

logistical challenges associated with leukapheresis scheduling, resource availability, limited CAR-T manufacturing slots and obligatory preinfusion release testing.[6] This can negatively impact treatment outcomes,[7] occasionally resulting in patients succumbing to their disease before treatment.[8] In addition, the necessary lymphodepletion prior to CAR-T infusion often leads to toxicity, placing a large burden on patients and the healthcare system.[9]

In recent years, in vivo CAR-T engineering has emerged as a promising alternative to ex vivo manufacturing approaches.[10] By directly modifying T cells within the patient, in vivo approaches could drastically increase accessibility and reduce both the wait times and costs currently associated with conventional CAR-T therapy, thereby significantly improving treatment options for many patients. However, this comes with its own challenges as T cells are inherently difficult to transfect or transduce, and effective T cell transfection requires activation while the majority of circulating T cells are in a resting state. Additionally, an in vivo CAR-T gene therapy vector must specifically target T cells while minimizing off-target uptake and transfection, as this may pose a safety concern.

Recently, several reports have described the successful development of targeted lentiviral vectors (LVs) for in vivo CAR-T engineering.[11–13] While promising, the use of LVs possesses disadvantages, including challenges in large-scale manufacturing[14] and safety concerns associated with insertional mutagenesis,[15] immunogenicity,[16] and the display of CAR protein on the LV envelope inducing off-target malignant cell transduction.[17] Non-viral delivery systems have gained considerable attention as a potentially safer and more accessible alternative.[18] Lipid nanoparticles (LNPs), in particular, have emerged as a promising candidate due to their relative ease of production and capacity to encapsulate and protect larger cargos in order to facilitate cellular uptake.[19] To date, most examples of in vivo T-cell engineering using LNP-based systems have focused on messenger RNA (mRNA) delivery.[20–23] While promising preclinical data have been generated with this strategy, it remains uncertain whether transient expression of CAR mRNA will be sufficient to achieve durable tumor control, as CAR-T cell persistence is required to sustain long-term efficacy.[24 25]

Here, we present a DNA-based strategy for in vivo CAR-T generation using a novel targeted LNP (tLNP) formulation, referred to as NCtx. This vehicle enables efficient, specific and functional delivery of DNA and mRNA to primary human T cells, leading to the generation of highly proliferative, functional and persistent CAR-T cells both in vitro and in vivo. A single intravenous injection of NCtx was capable of efficient in vivo CAR-T cell generation resulting in tumor control and extended survival in two distinct humanized mouse models using different CAR constructs. By overcoming key challenges faced by current CAR-T therapies, NCtx offers a novel alternative strategy to the evolving CAR-T therapy field, with the potential to improve accessibility and scalability of CAR-T-based treatments.

RESULTS

Development of a tLNP formulation for efficient codelivery of mRNA and mcDNA to T cells

To achieve stable DNA expression in T cells, we aimed to develop an LNP formulation capable of functionally codelivering both DNA and mRNA. This approach would enable the delivery of a DNA transgene template, flanked by transposase-compatible inverted terminal repeats, alongside mRNA encoding a transposase. This combination facilitates stable genomic integration of the delivered gene upon the transient expression of the transposase. We selected minicircle DNA (mcDNA) due to its absence of bacterial sequences and its smaller and more compact structure.[26]

While mRNA delivery to primary T cells using LNPs is well reported,[20–23] efficient DNA delivery remains a significant challenge, with limited reports on the use of non-viral nanoparticle-based methods for DNA transfection in T cells describing only modest levels of DNA transfection.[27–29] To test if LNPs could be used to transfect primary T cells with DNA, we formulated an LNP encapsulating both reporter mRNA (mCherry) and mcDNA (eGFP). We then applied this LNP to resting and preactivated T cells and transfection was assessed by flow cytometry. mcDNA could not be functionally delivered to T cells in resting or activated states as indicated by a lack of eGFP expression. Similarly to mcDNA, LNPs were also unable to functionally deliver mRNA to resting cells. However, in preactivated cells, a modest level of mCherry mRNA expression was observed (online supplemental figure 1).

To enhance transfection efficiency, we incorporated targeting moieties into the LNP formulation, as this strategy has been shown to improve LNP-mediated mRNA delivery to T cells.[20 21] CD7 was selected as a targeting ligand due to its broad expression on T cells and propensity for internalization.[30 31] Additionally, we explored the incorporation of an activating anti-CD3 single-chain variable fragment (scFv), hypothesizing that in addition to targeting, inducing T cell activation could further enhance functional DNA delivery to T cells. LNPs were functionalized using a previously described postinsertion method,[32] and were either left unmodified (untargeted), targeted with an anti-CD7 nanobody alone (tLNP-CD7), an anti-CD3 scFv alone (tLNP-CD3), or a combination of the two (tLNP-CD7/CD3). Both the untargeted and tLNPs exhibited favorable physicochemical properties, with particle sizes of around 100 nm, polydispersity indices of approximately 0.15, encapsulation efficiencies exceeding 95%, and an expected ratio of cholesterol to nucleic acid (online supplemental figure 2).

Incorporating CD3 or dual CD3/CD7 targeting into LNPs enabled functional mcDNA delivery to both resting and preactivated T cells as indicated by dose-dependent eGFP expression 4 days post-transfection (figure 1a).

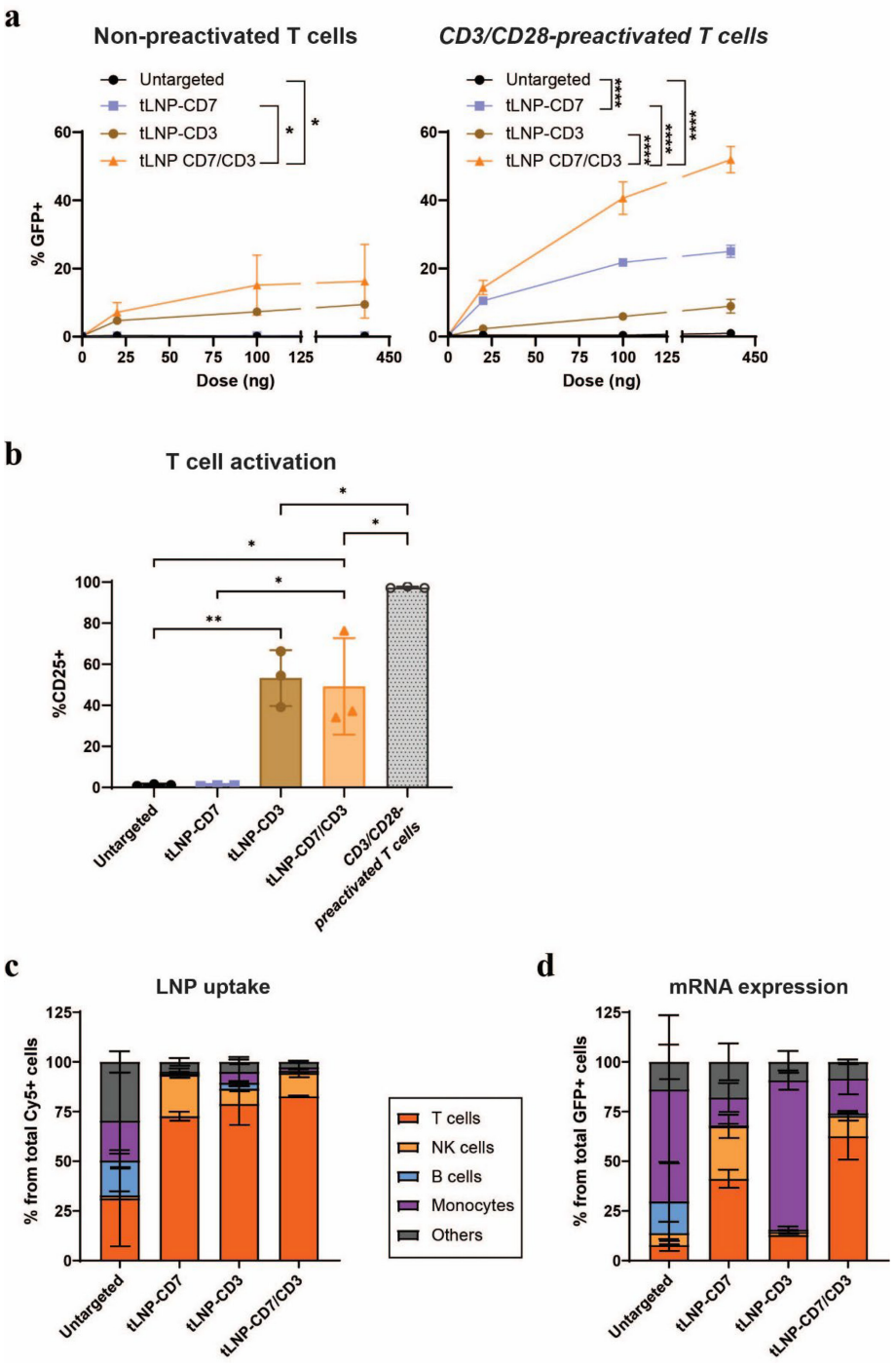

Figure 1 Dual-targeted anti-CD7/CD3 tLNPs functionally deliver mcDNA to T cells without exogenous activation while displaying high uptake and mRNA expression specificity. (a, b) Particles co-encapsulating reporter mCherry mRNA and eGFP mcDNA were either left unmodified (untargeted) or targeted with an anti-CD7 nanobody (tLNP-CD7), an anti-CD3 scFv (tLNP-CD3), or both (tLNP-CD7/CD3). These LNPs were applied to resting or CD3/CD28 bead preactivated T cells at a range of doses up to 400 ng total nucleic acid. (a) mcDNA expression after 96 hours shown as percentage eGFP+ cells measured by flow cytometry. (b) T cell activation status as measured by percentage of CD25+ cells by flow cytometry 96 hours post-treatment (400 ng dose). (a, b) n=3 T cell donors, data are mean±SD. (c, d) Surrogate particles co-encapsulating Cy5-labeled eGFP mRNA were applied to PBMCs at a dose of 20 ng to assess selectivity in a mixed cell population. (c) Uptake of the different LNP formulations was assessed after 2 hours as the percentage of each PBMC subset (T cells, NK cells, B cells, monocytes, and others) within the total Cy5+ population. (d) Functional mRNA delivery was evaluated after 24 hours as the percentage of each cell subset within the eGFP+ population. (d, e) n=2 T cell donors, data represent the mean±SD. P values were calculated using ordinary one-way ANOVA with Bonferroni correction for multiple comparisons. Where multiple doses were tested, statistics are calculated for the 100 ng dose. Only significant p values are plotted using *p<0.0332, **p<0.0021, ***p<0.0002 and ****p<0.0001. ANOVA, analysis of variance; LNP, lipid nanoparticle; mcDNA, minicircle DNA; mRNA, messenger RNA; NK, natural killer; PBMC, peripheral blood mononuclear cell; scFv, single-chain variable fragment; tLNP, targeted lipid nanoparticle.

While tLNP-CD7 did not facilitate mcDNA delivery to resting T cells, it efficiently transfected activated T cells, surpassing the efficacy of tLNP-CD3. Notably, the dual-targeted tLNP-CD7/CD3 exhibited the highest transfection efficiency in both resting and activated T cells, suggesting that CD3/CD7 cotargeting optimizes DNA delivery across different T cell activation states.

T cell activation following LNP transfection was assessed by CD25 expression. As shown in figure 1b, tLNP-CD3 and tLNP-CD7/CD3 induced T cell activation, whereas tLNP-CD7 transfection did not upregulate CD25 expression. These results, in conjunction with transfection data, indicate that T cell activation is necessary for efficient DNA delivery via LNPs. Additionally, all targeted LNP formulations effectively delivered mRNA to both resting and activated T cells, as evidenced by mCherry expression 24 hours post-transfection (online supplemental figure 3a). Notably, resting T cells transfected with tLNP-CD7 remained quiescent (figure 1b, online supplemental figure 3b), underscoring its potential for mRNA delivery without inducing activation.

In order to achieve effective in vivo T cell engineering, we hypothesized that the ability of our tLNP formulation to specifically transfect T cells while avoiding off-target cells would be of critical importance. Therefore, we evaluated the T cell specificity of the tLNPs by loading the particles with Cy5-labeled eGFP mRNA and applying them to human peripheral blood mononuclear cells (PBMCs). Particle uptake (Cy5) and mRNA expression (eGFP) in the different PBMC cell subsets was assessed after 2 or 24 hours respectively. Representative flow cytometry plots and gating strategy are shown in online supplemental figure 4. Analysis revealed significantly higher particle uptake in T cells relative to the total PBMC population for all tLNPs as compared with untargeted LNPs (figure 1c). Functional mRNA delivery showed that CD3 targeting alone was not sufficient to enhance expression specificity, which required the addition of CD7 targeting (figure 1d). While untargeted LNPs exhibited uptake and mRNA expression across multiple PBMC subsets, dual CD7/CD3 targeting resulted in preferential transfection of T cells. Notably, the addition of CD7 targeting to the LNPs also enhanced uptake and mRNA expression in natural killer (NK) cells, consistent with CD7 expression on this cell type. Although NK cells are not the primary target in this study, their transfection may be advantageous, as NK cells are increasingly explored as effector cells in CAR-based immunotherapies.[33]

In summary, our novel tLNP formulation can efficiently transfect T cells with both DNA and mRNA. CD7 targeting significantly enhanced mcDNA expression in activated T cells, while CD3 targeting allowed direct T cell activation, enabling mcDNA transfection without the need for exogenous stimulation. Moreover, CD7 targeting facilitated mRNA expression in resting T cells and ensured highly specific uptake and expression in target cells within a PBMC mixture. Together, these data suggest that our tLNP-CD7/CD3 vehicle possesses the necessary features for T cell-specific in vivo nucleic acid delivery.

NCtx generates functional and stable CAR-T cells in vitro using a CD19 CAR mcDNA construct

Building on our strategy for stable DNA expression in T cells, we developed NCtx, a tLNP formulation designed for stable in vivo CAR-T engineering by codelivering CAR-encoding mcDNA and SB100x transposase mRNA (figure 2a). To evaluate its potential for CAR-T generation, we formulated NCtx-CD19, encapsulating mcDNA encoding a CD19-specific CAR.

We first assessed NCtx-CD19's ability to deliver and integrate CAR mcDNA in preactivated T cells. Four days post-transfection, NCtx-CD19 induced CAR expression in over 41% of primary T cells whereas a control LNP lacking SB100x transposase resulted in only ~14% CAR+ cells (figure 2b). To demonstrate the generation of stable CAR-T cells, cells were cultured for 20 days. CAR signal in T cells treated with the non-transposase control particle fell to baseline after 7 days, while NCtx-CD19 enabled persistent signal with 21.8% of cells remaining CAR+ 20 days post-transfection (figure 2b,c).

To demonstrate that NCtx-CD19-engineered CAR-T cells were functional, they were co-cultured in vitro with CD19+ Nalm6 and Raji target cell lines at day 13 post-transfection at varying effector-to-target (E:T) ratios for 24 hours. Luciferase-based killing assays demonstrated robust, antigen-specific cytotoxicity as CD19+ target cells were killed by NCtx-CD19 CAR-T cells while the CD19– K562 control was not (figure 2d). Cytotoxic activity was associated with the upregulation of the proinflammatory cytokines interferon-gamma (IFN-γ) and interleukin 2 (IL-2) (figure 2e). The increased cytokine release was antigen-specific and observed only in transfected T cells, further confirming the functionality of NCtx-CD19-engineered CAR-T cells.

To function in vivo, it was important to confirm that NCtx-CD19 could also generate stable CAR-T cells without the addition of an exogenous source of activation as the majority of circulating T cells in the body are in a resting state. Again, NCtx-CD19 induced robust and long-term CAR expression in non-activated T cells, with CAR expression levels comparable to those in a CD3/CD28 bead-stimulated control (figure 2e).

Before initiating in vivo experiments, we first evaluated whether single LNPs were coloaded with both mRNA and mcDNA. We considered co-encapsulation to be important, as functional delivery of an LNP's cargo to a single cell is likely a rare event.[34] Ensuring both nucleic acid components are encapsulated within the same particle would significantly increase the likelihood of both nucleic acid components being found in the same cell, which would be required to achieve stable transfection. To assess coloading within individual particles, we employed three complementary analytical methods: advanced nano-flow cytometry,[35] a microscopy-based approach (EVquant),[36] and single particle automated Raman trapping analysis.[37]

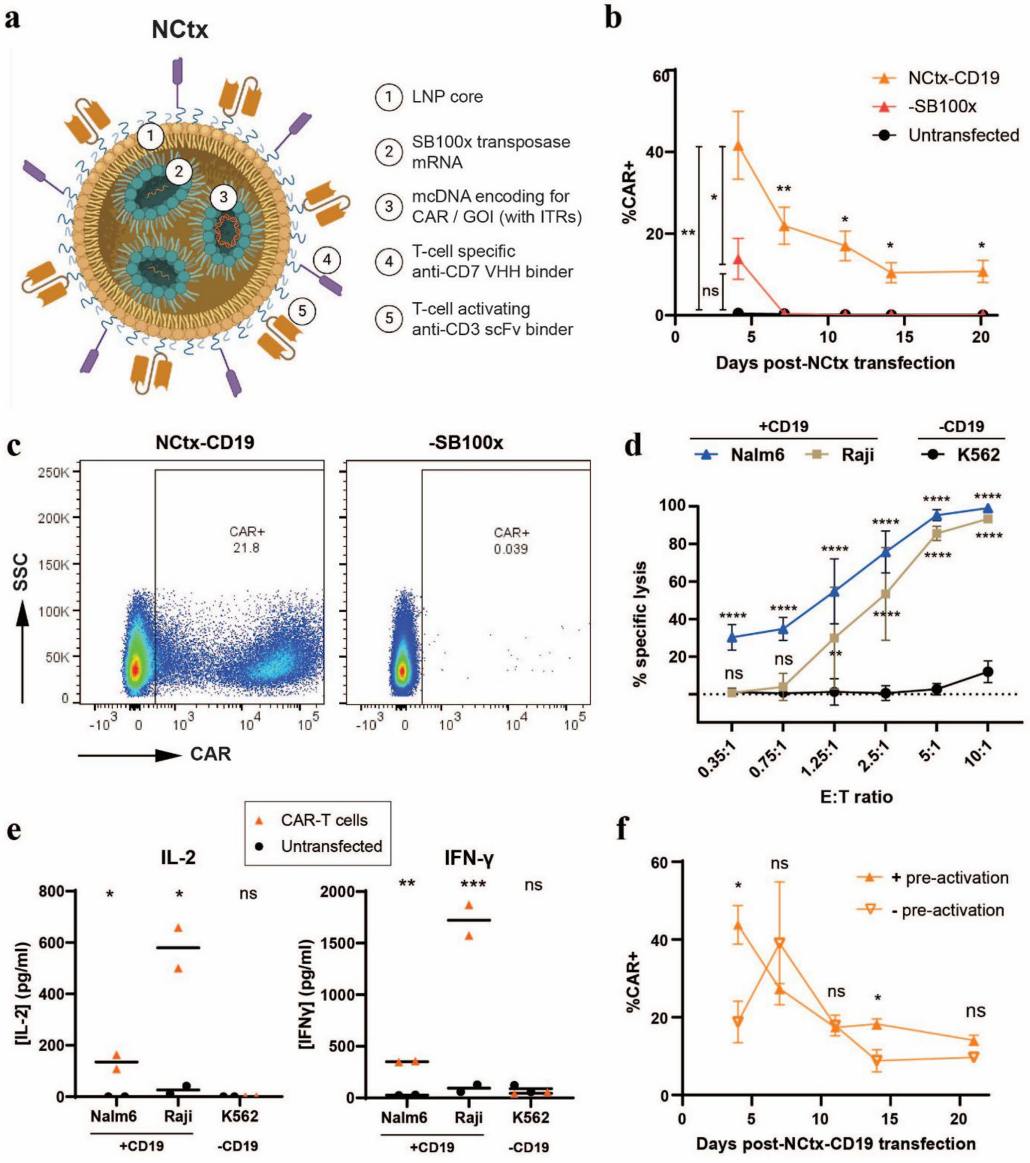

Figure 2 NCtx-CD19 generates stable and functional CAR-T cells in vitro. (a) Schematic representation of NCtx, a targeted LNP platform for T cell engineering. The LNP (1) encapsulates mcDNA encoding a CAR or another GOI flanked by SB100x-compatible ITRs (2), along with SB100x transposase mRNA (3) to mediate genomic integration of the GOI upon transient expression of the transposase mRNA. The vehicle is functionalized with anti-CD7 VHH (4) and anti-CD3 scFv (5) targeting ligands. (b, c) CD3/CD28 bead-activated T cells were treated with a dose of 800 ng total nucleic acid using NCtx-CD19, surrogate particles lacking SB100x mRNA transposase (–SB100x) or left untreated (untransfected) for 4 days. Cells were monitored over 20 days to evaluate stable genomic integration. (b) Transfection efficiency as the percentage of CD19 CAR+T cells as measured by flow cytometry at various time points post-transfection. n=9 different T cell donors, data represent the mean±SD. (c) Representative flow plots at day 14 are shown. (d) Antigen-specific cytotoxicity of NCtx-CD19-engineered CAR-T cells, measured via luciferase-based killing assays against CD19+ (Nalm6, Raji) and CD19-negative (K562) target cells. CAR-T cells were collected 13 days post-transfection and co-cultured with target cells at varying effector-to-target (E:T) ratios for 24 hours. Specific lysis was calculated relative to untransfected control cells. n=9 using different T cell donors, data represent the mean±SD. (e) Antigen-specific cytokine release by NCtx-CD19-engineered CAR-T cells, measured as the secretion of proinflammatory cytokines IL-2 and IFN-γ. Cytokines were measured after a 24-hour co-culture of effector and target cells at an E:T ratio of 2.5:1, using both CAR+ and untransfected T cells. n=1, measured in technical duplicates. (f) Transfection efficiency of resting (– pre-activation) and bead-activated (+ pre-activation) T cells at various time points post-transfection as measured by flow cytometry analysis of CD19-CAR+cells. n=2 T cell donors in two independent experiments, data are presented as mean±SD. P values were calculated using two-way ANOVA, mixed effect model with Tukey correction for multiple comparisons (b, d, f) or unpaired t-test (e). Significance is plotted with ns for p>0.0322 and *p<0.0332, **p<0.0021, ***p<0.0002 and ****p<0.0001. In (d) Nalm6 and Raji (CD19+) are compared with K562 (CD19–). ANOVA, analysis of variance; CAR, chimeric antigen receptor; GOI, gene of interest; IFN-γ, interferon-gamma; IL-2, interleukin 2; ITR, inverted terminal repeat; LNP, lipid nanoparticle; mcDNA, minicircle DNA; mRNA, messenger RNA; ns, not significant; scFv, single-chain variable fragment; SSC, side scatter; VHH, variable domain of a heavy-chain-only antibody.

Collectively, these orthogonal analyses suggested that a subset of LNPs successfully co-encapsulated both nucleic acid components (online supplemental figure 5).

NCtx-CD19 enables effective T cell transfection and sustained tumor control in a humanized in vivo model, achieving high functional efficacy

To evaluate the efficacy of NCtx-CD19 in vivo, we used a humanized B cell leukemia xenograft model, in which NXG immunodeficient mice were injected intravenously with luciferase-expressing Nalm6 tumor cells, followed by humanization with PBMCs (figure 3a). 7 days post-tumor injection, NCtx-CD19 was injected intravenously as a single dose of 0.5 mg total nucleic acid/kg. As a vehicle control, an NCtx particle encapsulating eGFP mcDNA and SB100x mRNA was administered at the same dose.

The CD19 CAR mcDNA transfection efficiency was assessed at multiple time points post-treatment. NCtx-CD19 administration resulted in robust and progressively increasing CAR expression in circulating T cells, reaching an average of 122 CAR+ T cells per µL of blood at 22 days postadministration (figure 3b). To confirm sustained CAR expression, splenic and bone marrow T cells were analyzed by flow cytometry. On day 24 post-NCtx-CD19 injection, an average of 24% of T cells from spleen and bone marrow expressed CAR in the treatment group (figure 3c). Exemplary flow cytometry plots are shown in online supplemental figure 6.

Additionally, tumor burden was monitored using bioluminescent imaging (BLI). Mice treated with the vehicle control particle exhibited rapid uncontrolled tumor growth. In contrast, mice treated with NCtx-CD19 demonstrated significant tumor control, reaching a plateau at day 21, followed by regression to baseline levels (figure 3d). These findings were further corroborated by significant differences in survival: all control mice succumbed to the tumor between days 24 and 28, whereas the majority of NCtx-CD19-treated mice survived until the study conclusion (figure 3e). The death of one mouse in the NCtx-CD19 group on day 17 occurred during anesthesia and was likely unrelated to tumor burden.

Next, we evaluated the potency of NCtx-CD19 in a dose de-escalation study in the same human PBMC engrafted mouse model, using a slightly modified setup (figure 3f). In this case, mice were treated 11 days post-PBMC injection with 4 or 40 µg/kg of NCtx-CD19 (125 or 12.5-fold lower compared with the previously used dose respectively) or a vehicle control encapsulating SB100x mRNA only. Remarkably, these lower doses of NCtx-CD19 still led to full (40 µg/kg) or partial (4 µg/kg) tumor control as shown by BLI measurements (figure 3g). This tumor control coincided with detectable CAR expression on T cells in blood, spleen and bone marrow at both doses (online supplemental figure 7).

These results highlight that NCtx-CD19 can stably transfect T cells in vivo across a broad dose range, leading to robust CAR expression on T-cells in circulation, spleen, and bone marrow, which translates into a sustained anti-tumor response.

NCtx enables CD19/CD22 dual CAR-T cell generation and tumor control in CD34+ HSC-engrafted NCG-His mice

We next replaced the CD19 CAR with a dual-specific CAR targeting both CD19 and CD22 (NCtx-dual). In this construct two nanobodies are fused in tandem via a flexible linker, followed by a transmembrane and a 41BB-CD3ζ signaling domain. This design was used to assess the versatility of the NCtx platform in functionally delivering and expressing more complex CAR constructs.

Similar to NCtx-CD19, NCtx-dual demonstrated strong in vitro efficacy, inducing stable CAR expression in both preactivated and resting T cells following transfection. Cytotoxic assays confirmed antigen-specific killing of CD19+and CD22+ single or dual-positive target cells, with cytotoxicity correlating with expression of the proinflammatory cytokine IFN-γ (online supplemental figure 8).

We next evaluated the in vivo efficacy of NCtx-dual using the same human PBMC-engrafted model previously employed for NCtx-CD19 in which a dose of 40 µg/kg total nucleic acid resulted in robust in vivo CAR-T generation and complete tumor elimination. Based on those findings, we selected a 50 µg/kg dose for NCtx-dual to assess its efficacy under comparable conditions. NCtx-dual induced a high frequency of circulating CAR-T cells (up to 50,000 CAR-T cells/µL of blood), achieved complete tumor clearance, and maintained durable CAR expression in T cells from the spleen and bone marrow (online supplemental figure 9). The exceptionally high number of circulating CAR-T cells observed is likely due to the enhanced T cell engraftment of the PBMCs used in this study, combined with the potent in vivo expansion of dual CAR-transfected T cells.

To further assess NCtx-dual in a more physiologically relevant setting, we employed the human CD34+ hematopoietic stem cell-engrafted NCG mouse model (NCG-His), which supports the development of a more diverse human immune cell population without the rapid occurrence of xenoreactivity typically observed in PBMC-engrafted animals. NCG-His mice were injected intravenously with 5×10^5 luciferase-expressing Nalm6 tumor cells, followed by intraperitoneal (IP) administration of 200 ng IL-7. Mice then received an intravenous injection of NCtx-dual or an NCtx vehicle control encapsulating eGFP mcDNA and SB100x mRNA at a dose of 50 µg/kg (figure 4a). Circulating T cells demonstrated robust transgene expression, with CAR-T cells appearing in circulation on day 14 and numbers increasing over time, reaching an average of 742 CAR-T cells/µL blood by day 40 postadministration (figure 4b). Tumor burden, monitored via BLI, showed exponential growth in control mice, whereas 7 out of 12 NCtx-dual-treated mice exhibited complete tumor elimination on day 42 (figure 4c). Importantly, treatment response seemed to correlate with T cell numbers pretreatment, with non or partial responders having lower numbers of circulating T cells

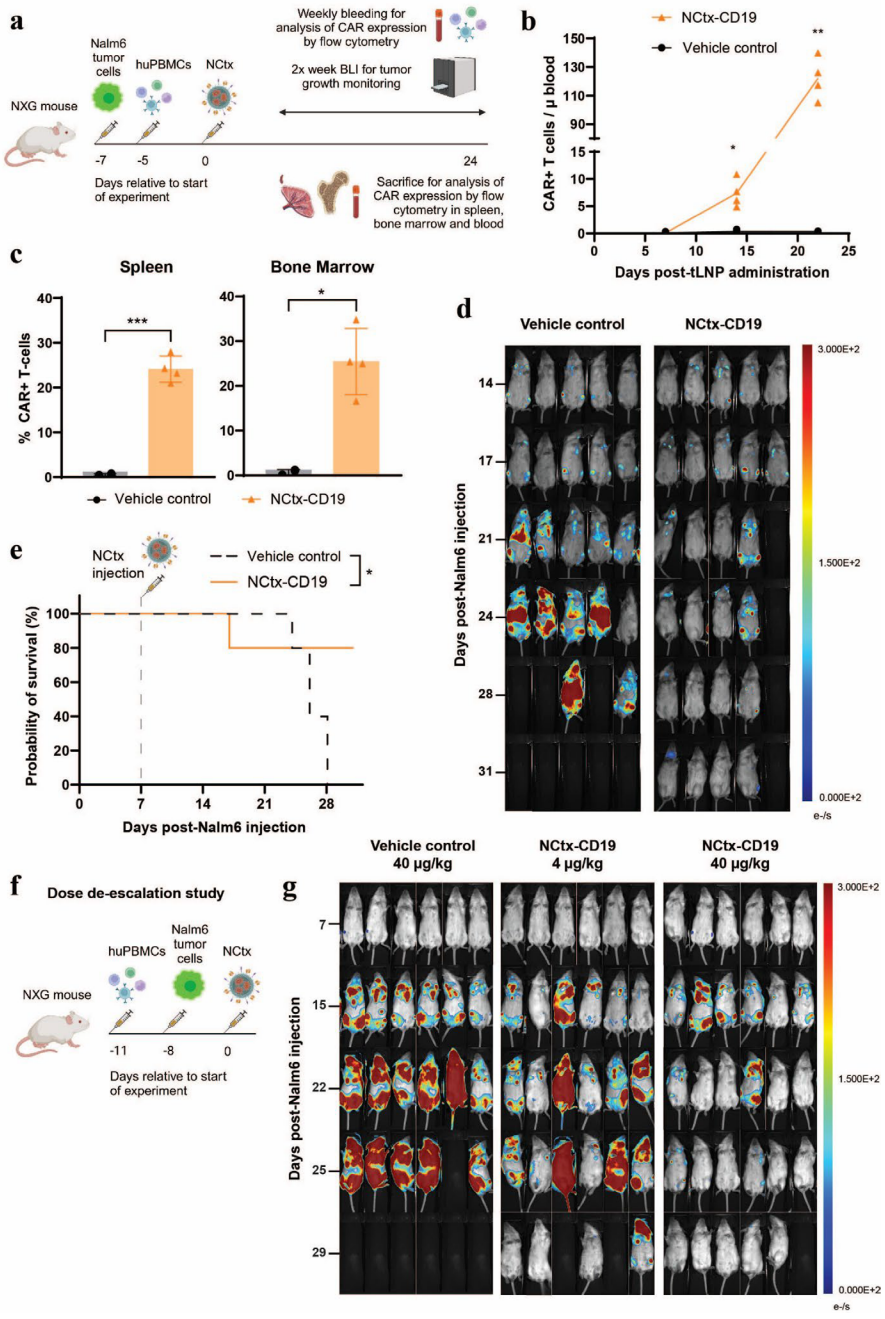

Figure 3 NCtx-CD19 generates CAR-T cells in vivo resulting in sustained tumor control across a range of doses in a human PBMC model of leukemia. (a) Schematic representation of study timeline: NXG mice were injected intravenously with 5×10^5 luciferase-expressing Nalm6 tumor cells, followed by humanization with 5×10^6 huPBMCs. NCtx-CD19 or a NCtx surrogate encapsulating eGFP mcDNA and SB100x mRNA (vehicle control) were administered intravenously at a total nucleic acid dose of 0.5 mg/kg. (b) Transfection efficiency in circulating T cells was measured over time via flow cytometry, represented as CAR+ cells/µL of blood. n=4 (NCtx-CD19) or n=5 (vehicle control), data are mean with individual values plotted. (c) CD19 CAR mcDNA expression was assessed by flow cytometry in spleen and bone marrow at the study's end. Vehicle-treated mice reached HEP and were analyzed between days 24–28 (n=2), while NCtx-CD19-treated mice were all terminated and analyzed on day 31 (n=4). Data are presented as mean±SD. (d) Nalm6 tumor burden was monitored by BLI. (e) Kaplan-Meier survival analysis. Mouse death in the NCtx-CD19 group on day 24 post-Nalm6 was due to anesthetic overdose, unrelated to health or tumor burden. n=5. (f) Schematic representation of the dose de-escalation study timeline: NXG mice were humanized with 5×10^6 huPBMCs 11 days pre-LNP injection, followed by intravenous injection with 5×10^5 luciferase-expressing Nalm6 tumor cells 8 days before treatment. NCtx-CD19 or a NCtx vehicle control encapsulating only SB100x mRNA (vehicle control) were administered intravenously at a dose of total nucleic acid of either 40 or 4 µg/kg. (g) Nalm6 tumor burden was monitored via BLI. P values were calculated using two-way ANOVA, mixed effect model (b), unpaired t-test (c) or log-rank Mantel-Cox test (e). Significance is plotted *p<0.0332, **p<0.0021 and ***p<0.0002. ANOVA, analysis of variance; BLI, bioluminescent imaging; CAR, chimeric antigen receptor; HEP, humane endpoint; LNP, lipid nanoparticle; mcDNA, minicircle DNA; mRNA, messenger RNA; PBMC, peripheral blood mononuclear cell; tLNP, targeted lipid nanoparticle.

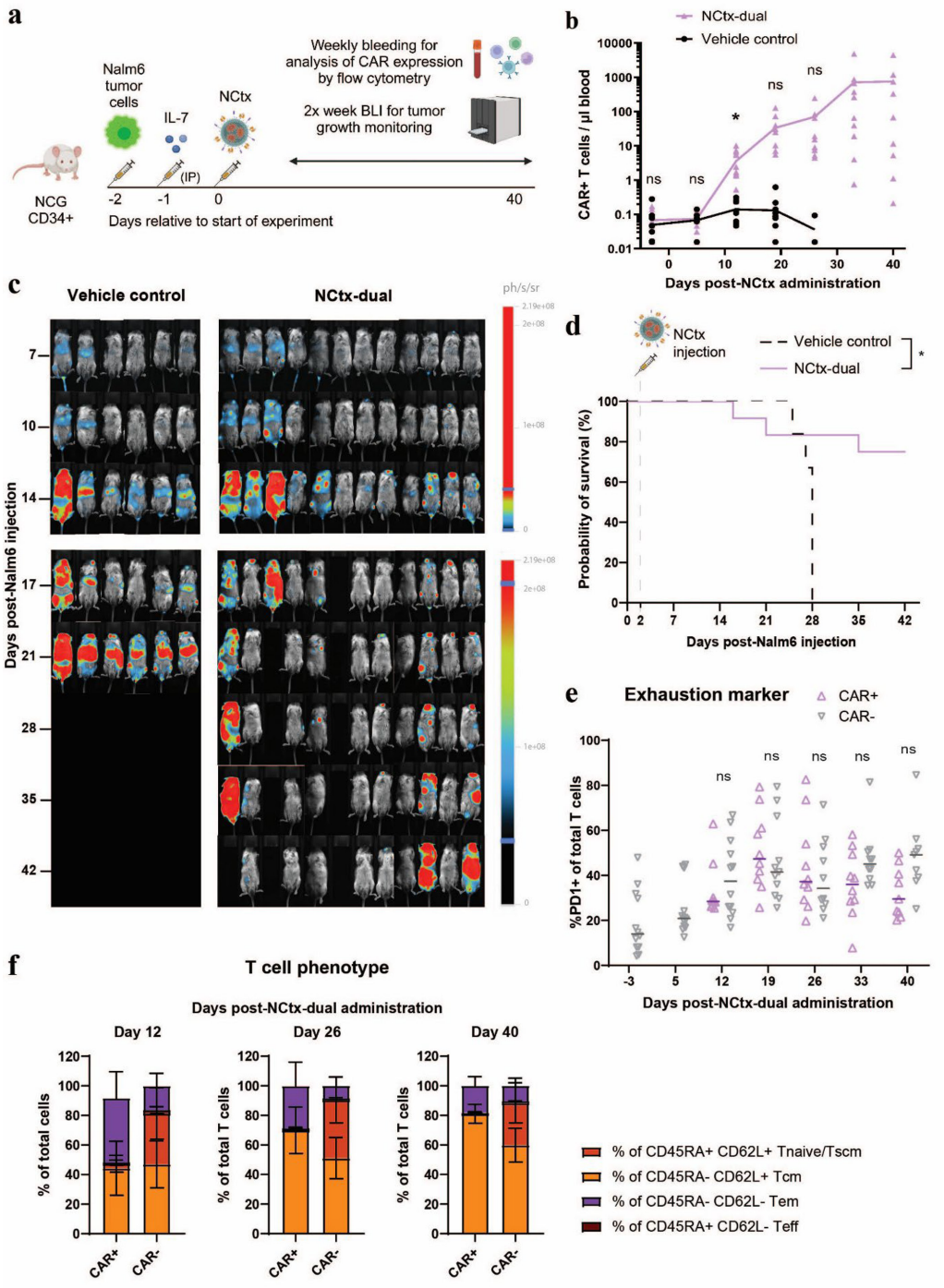

Figure 4 NCtx-dual induces robust and durable in vivo CAR-T generation, tumor control and extended survival in CD34+ HSC-engrafted NCG mice. (a) Schematic representation of study design: NCG mice engrafted with CD34+ HSC (NCG-His) were injected intravenously with 5×10^5 luciferase-expressing Nalm6 tumor cells, followed by IP injection of 200 ng IL-7. Mice were treated intravenously with NCtx-dual or a NCtx vehicle control encapsulating eGFP mcDNA and SB100x mRNA (vehicle control) at a total nucleic acid dose of 50 µg/kg. (b) CD19/CD22 dual CAR mcDNA expression was assessed by flow cytometry in circulating T cells for 40 days post-NCtx administration. n=12, data are presented as mean with individual values. (c) Nalm6 tumor burden was monitored by BLI. (d) Kaplan-Meier survival analysis. n=6 (vehicle control) or n=12 (NCtx-dual). (e) Expression of the exhaustion marker PD-1 in CAR+ and CAR– T cell populations over time in NCtx-dual-treated mice, analyzed by flow cytometry. n=12, data represent mean±individual values. (f) T cell phenotype characterization (Tnaive/Tscm, Tcm, Tem, and Teff) based on CD45RA and CD62L expression in CAR+ and CAR– T cells after NCtx-dual administration. n=12, data represent mean±SD. P values were calculated using log-rank Mantel-Cox test (b) or two-way ANOVA, mixed effect model (d, e). Significance is plotted with ns for p>0.0332 and *p<0.0332. ANOVA, analysis of variance; BLI, bioluminescent imaging; CAR, chimeric antigen receptor; HSC, hematopoietic stem cell; IL-7, interleukin 7; IP, intraperitoneal; mcDNA, minicircle DNA; mRNA, messenger RNA; ns, not significant; PD-1, programmed cell death protein-1; Tcm, central memory T cell; Teff, effector T cell; Tem, effector memory T cell; Tnaive, naïve T cell; Tscm, stem cell memory T cell.

prior to treatment compared with complete responders (online supplemental figure 10), reinforcing the necessity of sufficient T cell presence for in vivo CAR-T generation. Consistent with effective in vivo CAR-T activity, we also observed sustained depletion of circulating CD19+B cells in treated animals, providing additional evidence of antigen-specific cytotoxicity beyond the Nalm6 tumor model (online supplemental figure 11). Kaplan-Meier survival analysis confirmed a significant survival benefit in NCtx-dual-treated mice, with all control mice succumbing by day 28, while 75% of treated mice survived until day 42 (figure 4d).

Flow cytometry analysis of the T cell exhaustion marker programmed cell death protein-1 (PD-1) expression revealed no clear sign of CAR T-cell exhaustion, as PD-1 levels in CAR+ and CAR− T cells were equal over time in the NCtx-dual treatment group (figure 4e). Additionally, T cell differentiation profiling based on CD45RA and CD62L expression showed a mixed central memory T cell (T_{CM}) / effector memory T cell (T_{EM}) phenotype at day 12 after transfection, which shifted by day 40 toward a less differentiated, more favorable T_{CM} phenotype that is associated with increased CAR-T persistence and complete response in CAR-T treated patients[38] (figure 4f).

These findings demonstrate that NCtx-dual enables effective in vivo CAR-T generation in a CD34+ humanized model. The robust expansion and favorable memory phenotype of NCtx-dual-derived CAR-T cells correlated with sustained tumor control and improved survival, highlighting the potential of NCtx as a novel non-viral platform for in vivo CAR-T therapy.

DISCUSSION

Together, these findings demonstrate that our newly developed tLNP, NCtx, can cotransfect T cells with both DNA and mRNA, thereby allowing the generation of functional and stably expressing CAR-T cells both in vitro and in vivo with an efficiency unprecedented for a non-viral DNA gene therapy vector. By generating CAR-T cells directly in the patient, in vivo CAR-T approaches such as NCtx have the potential to bypass the complex manufacturing and logistical challenges which currently prevent the widespread use of CAR-T therapy. This promises to revolutionize and democratize CAR-T treatment, making this therapy accessible to all patients who might benefit from it.

A crucial aspect of NCtx is its targeting, which not only enhanced particle specificity and mRNA transfection efficiency but was also essential for DNA delivery to primary T cells. In the absence of CD7 or CD3 targeting, particles were completely incapable of functional DNA delivery; this capability was only conferred on the addition of the selected binders. Our data suggest that CD7 is a highly advantageous target for nucleic acid delivery, as tLNP-CD7 outperformed tLNP-CD3 for DNA delivery to preactivated T cells and was capable of functionally delivering mRNA to fully resting T cells while preserving their quiescent state; a notable advantage since T cell transfection typically requires prior activation. By combining CD7 targeting with an anti-CD3 activating binder, we generated a tLNP that efficiently codelivers mRNA and DNA to primary T lymphocytes in vitro and in vivo without the need for additional T cell stimulation.

There are few other examples of non-viral and non-electroporation-based DNA delivery methods for T cells. Most of these examples make use of polymer-based systems which have not been tested in vivo.[28 29] To our knowledge, the only comparable example of a T cell-targeted non-viral DNA vector is provided by Smith *et al*,[27] who developed a poly-(β-amino ester)-based nanoparticle capable of achieving 3.8% CAR expression in vitro. This vector generated functional CAR-T in vivo but required repeat administration on five consecutive days and was only capable of generating roughly 10 CAR-T cells/µl peripheral blood in contrast to the >100 CAR-T cells/µl generated by a single administration of NCtx-CD19 or NCtx-dual. The lack of reported advancements in in vivo CAR-T using polyplex nanoparticles in recent years highlights the challenges faced by this class of nanoparticle.

An example of functional CAR-T generation in vivo using LNPs is provided by Billingsley *et al* who developed CD3 or CD7 targeted LNP formulations containing CAR mRNA.[21] These formulations were capable of generating significant CAR expression in circulating T cells 12 and 36 hours post-LNP administration which was associated with modest B cell ablation. However, 60 hours postadministration, CAR expression returned to almost baseline levels. Although impressive, this particle does not appear to be capable of achieving the prolonged expression shown by the DNA-based NCtx. Furthermore, Billingsley *et al* required a dose of 2 mg nucleic acid/kg to generate significant CAR expression which persisted only 60 hours postadministration. In contrast, NCtx-CD19 at 40 µg/kg and NCtx-dual at 50 µg/kg each induced high levels of circulating CAR-T cells, which persisted for several weeks and led to complete tumor control. The dose used by Billingsley *et al* is typical for in vivo T cell engineering using mRNA-containing LNPs,[23] yet it is 50-fold higher than the lower doses successfully used in our study. This further highlights NCtx's efficacy and aids in alleviating concerns relating to toxicity as the NCtx dose required for a functional response is considerably lower than those used by clinically evaluated mRNA LNP formulations such as Moderna's mRNA-3705, which is dosed at 600 µg/kg.[39]

With the functional and specific codelivery of mcDNA and transposase mRNA to T cells using a single particle, NCtx can achieve stable in vivo CAR-T generation with an efficacy on par with previously published viral vector-based in vivo CAR-T strategies.[11 13] These therapies have shown promising preclinical data, and are now moving to a clinical testing phase.[40] Manufacturing of lentiviruses is however a costly and cumbersome process that is not easily scalable,[41] potentially limiting the broad application of these vectors for in vivo CAR-T engineering. It is possible that although effective, viral vector-based methods of in

vivo CAR-T will be hindered by similar complex manufacturing and logistical constraints which currently prevent the widespread utilization of ex vivo CAR-T therapies. In contrast, NCtx, an LNP-based vehicle, will likely have better manufacturability resulting in a more cost-effective and accessible non-viral alternative.

Another advantage of the NCtx system in comparison to viral vector-based methods is its increased safety. Gene therapy is associated with inherent risk for insertional mutagenesis, however, in comparison to lentiviral, retroviral and other transposon-transposase systems, the SB100 transposase has been shown to be relatively safe. Studies have shown that SB100 has a close to random integration pattern with a lower tendency to integrate into genes and regulatory sequences compared with viral vectors, coinciding with a higher chance of integrating in safe harbor loci.[42] Additionally, due to the production process of CAR-T lentiviruses, CARs are displayed on the envelope of lentiviruses. This phenomenon is reported to promote the transduction of target antigen-expressing cells.[17] When LVs are used for in vivo gene therapy this phenomenon poses an additional risk for off-target malignant cell transduction, as malignant B cells cannot be separated from the intended target cells prior to treatment, as is custom for ex vivo CAR-T manufacturing.

In summary, our study demonstrates that the novel combined CD3/CD7 targeting system employed here confers NCtx with the ability to stably transfect T cells with DNA with an efficiency unique for a non-viral vector. This ability allows NCtx to achieve efficient, stable, and functional in vivo CAR-T cell generation. To our knowledge, this is one of the first reports showing efficient non-viral DNA delivery to T cells in vivo, positioning NCtx as a promising advancement in the field of in vivo CAR-T therapy. Compared with current ex vivo and other in vivo CAR-T approaches, NCtx offers key advantages, including reduced costs, simplified logistics, improved accessibility and reduced turnaround times for patients. Further development of this novel gene therapy vehicle is important, including a deeper investigation into the mechanistic basis for the enhanced transfection efficiencies observed, as well as validation in additional relevant preclinical models.

MATERIALS AND METHODS

Nucleic acid production

mcDNA was produced according to Mayrhofer *et al* in 2018.[43] In short, mcDNA was produced in *E. coli* TB1 grown in Terrific Broth (TB) medium supplemented with 50 µg/mL kanamycin and purified using the NucleoBond Xtra Maxi Plus EF kit (Macherey-Nagel, 740426) according to the manufacturer's instructions for low-copy plasmids. Purity was analyzed using agarose gel analysis (Biotium, 41003). For in vivo experiments, mcDNA was further purified using the Norgen endotoxin removal kit (21900). SB100x mRNA was produced in-house with the VENI all-in-one mRNA Synthesis Kit with Cap1 Analog (Leish Bio, R1001.3). To obtain the template for the in-vitro transcription (IVT) reaction, the gene of interest was amplified by PCR reaction with a primer containing a poly(A) tail and the product was purified using a standard PCR purification kit. This product was transcribed by the T7 RNA polymerase, resulting in Cap 1 capped N1-methyl-pseudoUTP RNA. After removing the DNA template using DNase (Invitrogen, AM2239) at 37°C for 30 min, a short centrifugation was performed to remove pyrophosphate. The mRNA in solution was precipitated o/n at −20°C using the precipitation reagent provided with the IVT kit. The following day the precipitated mRNA was washed with 70% ethanol before proceeding with purification using the MEGAclear Transcription Clean-Up Kit (Invitrogen, AM1908).

LNP production

Lipid stock solutions were prepared in ethanol. An ionizable lipid stock of 20 mg/mL was prepared along with helper lipid, cholesterol and Polyetyleenglycol (PEG)-lipid stocks at 10 mg/mL. Lipid stock solutions were warmed to 37°C for 20 min before use. LNP formulations consisted of ionizable lipid/helper lipid/cholesterol/PEG-lipid at appropriate ratios. Ionizable lipids used were either obtained from the lab of Yusuke Sato (Hokkaido University) or were commercially sourced from Avanti Research. Nucleic acid cargo consisted of mcDNA and SB100x transposase mRNA at a 1:1 w:w ratio unless otherwise stated. Nucleic acid mixes were diluted in 100 mM acetate buffer (pH 4). Lipid mixes were diluted to 5 mM total lipid in absolute ethanol and mixed with nucleic acid using a Nanoassemblr Benchtop microfluidic mixing system (Precision Nanosystems) at a flow rate ratio of 2:1 (aqueous:lipid) using a total flow rate of 6 mL/min. The total volume of LNP produced ranged from 800 µl to 5 mL. All LNP productions were performed at room temperature. Immediately after production, LNP mixes were stored on ice. After production, LNPs were dialyzed overnight into phosphate-buffered saline (PBS) (pH 7.4) at 4°C using 20 KDa G2 dialysis cassettes (Thermo Fisher).

LNP targeting

Anti-CD7 nanobody was obtained from a phage library obtained from QVQ Holding BV, after immunization of two llamas with mRNA encoding for full-length human CD7 antigen. Panning was performed using CD7-expressing Flp-In T rex cells (Invitrogen) generated using manufacturer's instructions. Individual selected clones were further validated and tested for binding using ELISA and flow cytometry. The selected CD7 nanobody clone and anti-CD3 scFv (UCHT-1) were fused to a C-terminal tag including a cysteine for conjugation to PEG-lipid and an EPEA peptide sequence for affinity purification. The anti-CD7 nanobody was produced in yeast cells (Saccharomyces cerevisiae) by QVQ, the anti-CD3 scFv was produced in HEK293E cells by ImmunoPrecise Antibodies. Anti-CD7 nanobody and anti-CD3 scFv binders were conjugated to 1,2-distearoyl-sn-glycer

o-3-phosphoethanolamine (DSPE)-PEG-Maleimide via a C-terminal cysteine by overnight incubation in PBS at a 1:1 lipid:protein ratio. Binder-lipid conjugates were then postinserted onto the particles as described by Swart *et al*.[32] After postinsertion, targeted LNPs were dialyzed overnight into PBS (pH 7.4) using 20 KDa G2 dialysis cassettes (Thermo Fisher).

LNP characterization

The size and polydispersity of LNP preparations were analyzed using dynamic light scattering performed at a fixed angle of 173° using a Nano S Zetasizer instrument (Malvern Panalytical) equipped with a 4 mW HeNe laser of 633 nm. Samples were diluted to a concentration of 1 ng/µl in PBS and measured at 25°C for 30 s at least 10 times. To determine the nucleic acid concentration and encapsulation efficiency, the Quant-iT RiboGreen assay (Thermo Fisher) according to manufacturer's instructions was performed using a standard curve consisting of mcDNA and SB100x mRNA at the exact ratio found in the LNP particle being analyzed.

Primary cell culture and in vitro transfection

First, PBMCs were isolated from healthy donor blood using Ficoll-Paque (GE Healthcare) and SepMate PBMC isolation tubes (STEMCELL) according to manufacturer's instructions. T cells (including CD3+ CD4+ and CD3+ CD8+ cells) were then isolated from the PBMCs using an EasySep Human T cell isolation kit (STEMCELL) according to manufacturer's protocol. PBMCs or T cells were plated in a 96-well F-bottom plate in T cell medium (Roswell Park Memorial Institute (RPMI) 1640 (Gibco), 2.5% human Serum (Sanquin), 1% Pen/Strep (Invitrogen) supplemented with 50 iU/mL IL-2 (Miltenyi Biotec) and 1 µg/mL Apo lipoprotein-E (Abcam). If indicated, the T cells were preactivated by CD3/CD28 dynabeads (Gibco) at a 1:1 bead to T cell ratio. LNPs were added at the dose of total nucleic acid indicated and incubated for 96 hours for DNA transfection, 24 hours for mRNA transfection and two or 4 hours for uptake. McDNA transfection efficiency was assessed using mcDNA encoding either CD19 CAR or eGFP. mRNA expression was assessed using the expression of mCherry reporter mRNA. LNP uptake was measured using LNPs loaded with mRNA conjugated to Cy5.

Cell lines

Target cell lines expressing firefly luciferase were either generated *in-house* or obtained from commercial suppliers. K562 cells (ACC 10) were sourced from DSMZ GmbH and modified *in-house* to stably express firefly luciferase and mCherry separated by p2A. Nalm6 (CL-1660) and Raji (CL-1212) cell lines were procured from FenicsBIO. All cell lines were cultured in RPMI medium supplemented with 10% fetal calf serum (FCS) and 1% penicillin-streptomycin.

To further characterize the dual CAR targeting CD19 and CD22, Nalm6 knockout cell lines lacking either CD19 (Nalm6 KO*), CD22 (Nalm6 KO**), or both (Nalm6***) were generated using the CRISPR/Cas9 system. LVs expressing CRISPR/Cas9 and guide RNAs (gRNAs) were procured from VectorBuilder and used to transduce Nalm6 cells stably expressing firefly luciferase (CL-1660), at a multiplicity of infection (MOI) of 10. The mammalian CRISPR LV for a single guide RNA (sgRNA) (VectorBuilder) was used, which contains both the cassette for Cas9 and sgRNA expression on the same vector. The human codon-optimized Cas9 (hCas9) cassette consisted of an elongation factor-1 alpha short (EFS) promoter, a hCAS9-P2A-puromycin resistance (puroR) coding sequence and woodchuck hepatitis virus posttranscriptional regulatory element (WPRE). The sgRNA expression cassette consists of a U6 promoter, the sgRNA sequence and a RNA polymerase III (Pol III) transcription terminator. The sgRNA target sequences for human CD19 and CD22 knockout were derived from the Brunello library,[8 44] and are as follows: CD19: 5'-GGAAAGTATTATTGTCACCG-3', CD19: 5'-CTAGGTCCGAAACATTCCAC-3', CD22: 5'- ATTCATACCGGGTAACACTG-3', CD22: GGTATCCGATCCAATTGCAG. Two targets per gene were used to increase the chance of successful gene knockout. Transduced cells were maintained in culture and monitored for knockout efficiency by assessing antigen expression via flow cytometry. To obtain a homogeneous knockout population, cells were bulk sorted using a Sony MA900 cell sorter.

Flow cytometry

CD19 CAR expression in in vitro experiments was detected using CD19 CAR detection reagent (Miltenyi Biotec, REA1297, 1:400) and streptavidin-APC-Cy7 (BD, REA746, 1:200), CD19/CD22 dual CAR expression was detected using CD22 CAR detection reagent (Miltenyi Biotec, 130-126-727, 1:1000) and streptavidin-APC-Cy7 (BD, REA746, 1:200). T cell activation status was assessed using anti-huCD25-APC (CD25-4e3) (Thermo Scientific, 17-0257-42, 1:200) and anti-huCD69-PE-Cy7 (FN50) (Miltenyi, 130-112-615, 1:100). For specificity experiments using PBMCs a ZombieAqua (BioLegend) live:dead stain was applied along with an Fc Block (BD, 564220, 1:200). Cell types were then identified within the PBMC mix using anti-huCD2-BV605 (S5.2) (BD, 745205, 1:1000) and anti-huCD8-PE-Cy7 (BioLegend, 344702, 1:1000) to identify T cells, anti-huCD56-BV786 (BD, 564058, 1:200) to identify NK cells, anti-huCD19-PE (A3-B1) (Antibodies online, ABIN1112077, 1:100) to identify B cells and anti-huCD14-BV650 (M5E2) (BioLegend, 301836, 1:200) to identify monocytes.

For the analysis of most in vivo samples, a ZombieAqua (BioLegend) live:dead stain was applied along with an Fc Block (BD, 564220, 1:200). For the analysis of CD19 CAR expression in in vivo samples CD19 CAR detection reagent (Miltenyi Biotec, REA1297, 1:400) and streptavidin-APC-cy7 (BD, REA746, 1:200) were used. CD19/CD22 dual CAR expression was detected using CD22 CAR detection reagent (Miltenyi Biotec,

REA130-126-727, 1:1000) and streptavidin-APC-Cy7 (BD, REA746, 1:200). Cell types were identified using anti-huCD3-PB (HIT3A) (BioLegend, 557597, 1:400) and anti-huCD8-PE-Cy7 (BioLegend, 344702, 1:1000) to identify T cells, anti-huCD56-BV786 (BD, 564058, 1:200) to identify NK cells, anti-huCD19-PE (A3-B1) (Antibodies online, ABIN1112077, 1:100) to identify B cells and anti-huCD14-BV650 (M5E2) (BioLegend, 301836, 1:200) to identify monocytes. Anti-huCD45- APC-Vio770 (5B1) (Miltenyi, 130-113-115, 1:250) was also used to differentiate human leukocytes from murine cells.

For the analysis of the in vivo samples performed by TransCure bioServices (figure 4), CD19/CD22 dual CAR expression was detected using CD22 CAR detection reagent (Miltenyi Biotec, REA130-126-727, 1:1000) and biotin-APC (Miltenyi Biotec, REA746, 1:200). Viability was determined with live/dead FVS780 stain (BD, 565388). The different cell types and T cell exhaustion or differentiation markers were identified with the following antibodies: PD-1-BV421 (BioLegend, 329920), CD56-BV510 (362534), human CD45-BV605 (BD, 564047), CD14-BV711 (BioLegend, 301838), CD3-BV786 (BD, 563800), CD45RA-FITC (BioLegend, 304806), CD4-PerCPVio700 (Miltenyi, 130-113-218), CD62L-PE (BioLegend, 304806), CD19-PE Dazzle594 (BioLegend, 302252) and CD8-PE Cy7 (BioLegend, 344712).

Flow cytometry analysis was performed using either a Canto or LSRFortessa flow cytometer (BD). Data analysis was performed using FlowJo software.

Functional T cell assays

A luciferase-based killing assay was performed to evaluate the functionality of NCtx-engineered CAR T cells against CD19+ target cells (NCtx-CD19) or CD19+ and CD22+ single or dual-positive target cells (NCtx-dual). Prior to the assay, CAR expression was confirmed and only CAR+ T cells were counted as effectors. On day 13 or 14 post-transfection, CAR T cells were co-cultured with 5,000 target cells: K562, Raji and Nalm6 (NCtx-CD19) or Nalm6, Nalm6 KO* (CD19− CD22+), Nalm6 KO** (CD19+ CD22−) and Nalm6 KO*** (CD19− CD22−) (NCtx-dual) at varying E:T ratios (3:1, 1.5:1, 0.75:1, and 0.35:1) for 24 hours. Before measurement, Luciferin (Abcam) was added to each well and luminescence was measured using a SpectraMax iD3 device. Cell numbers were normalized to CAR expression, and untreated T cells from the same donor were used as negative controls.

In vivo models

Study conducted in France

The animal experiment described in figure 4 was conducted by TransCure bioServices. This study was performed under the authorization of the French Ministry of Higher Education, Research, and Innovation (approval no. 38 383–2022082413416895) and the Departmental Directorate for the Protection of Populations in Haute Savoie (approval no. A 7418 324), and in accordance with the Association for Assessment and Accreditation of Laboratory Animal Care International (AAALAC International) accreditation (reference no. 001909). Female specific opportunist and pathogen-free (SOPF) NOD-Prkdc^{em26Cd52}Il2rg^{em26Cd22} immunodeficient (NCG) mice were obtained from Charles River, housed under SOPF conditions at TransCure bioServices, and engrafted with human cord blood-derived CD34+ stem cells (NCG-HIS). Only mice with a humanization rate (hCD45/total CD45) above 25% were used. Mice were kept at 22±2°C and 55±10% hygrometry conditions, on a 12 hours light 12 hours dark regimen in an individually ventilated cage system. Mice were fed with sterile food and water ad libitum. Mice were injected with 500,000 Nalm6-luciferase cells in 100 µl of PBS 2 days prior to NCtx injection as indicated in the figure caption (figure 4a). 200 ng of IL-7 (Miltenyi Biotec) in 100 uL PBS was injected IP 1 day prior to NCtx injection. NCtx particles were diluted in 20 mM Tris, 5 mM NaCl, 8% Sucrose pH 7.4 and 100 µl of particle was injected via tail vein injection at the total mg nucleic acid per kilogram of mouse dose indicated. Tumor outgrowth was assessed by BLI imaging over the course of the following 7 weeks post-NCtx injection once or two times a week. Shortly, mice were anesthetized with isoflurane and injected IP with 2.5 mg of luciferin (Promega) in 100 µl PBS prior to imaging with Vilber NEWTON V.7.0. CAR expression in blood was assessed using flow cytometry analysis of between 20 µl and 100 µl blood obtained from the tail vein at weekly intervals. Humane endpoints were agreed on with the ethics committee and were defined by Transcure bioServices' clinical scoring system.

Studies conducted in The Netherlands

The rest of animal experiments were performed with the Animal Welfare Body Utrecht's permission and complied with the Dutch Experiments on Animals Act (WOD) under license AVD11500202316783. The research was carried out in accordance with the Guide for the Care and Use of Laboratory Animals. Mice were randomly assigned to experimental groups using the randomization function in Excel. Blinding was implemented by researchers who were not involved in animal handling. Female NOD-*Prkdc^{scid}Il2rg^{tm}*/Rj (NXG) or NXG-mice engrafted with cord blood-derived human CD34+stem cells (NXG-HIS), were obtained from Janvier and were housed under sterile conditions at the Central Animal Facility of Utrecht University. Experiments were performed according to institutional guidelines after permission was obtained from the Animal Welfare Body Utrecht (16783-1-04, 16783-3-05, 16783-3-06, 16783-3-09). Mice were kept at 45–65% humidity on a 12 hours light 12 hours dark regimen in an individually ventilated cage system. Mice were fed with sterile food (V1534-703, Ssniff).

NXG mice were between 1–3 months and NXG-HIS CD34+ mice were around 6 months to 7 in age at the start of experiments. NXG mice were humanized via tail vein injection of 5,000,000 human PBMCs in 100 µl of PBS either 11 or 5 days prior to NCtx injection as indicated in figure captions. Mice were injected with 500,000 Nalm6-luciferase cells in 100 µl of PBS 7 or 8 days prior to LNP injection as indicated in figure captions. LNPs were diluted in PBS or 20 mM Tris, 5 mM NaCl, 8% Sucrose pH 7.4 and between 80 and 120 µl of LNP dilution was injected via tail vein injection at the total mg nucleic acid per kilogram of mouse dose indicated. Tumor outgrowth was assessed by BLI imaging over the course of the following 4–7 weeks post-NCtx injection once or two times a week. Shortly, mice were anesthetized with isoflurane and injected IP with 2.5 mg of luciferin (Promega) in 100 µl PBS prior to imaging. CAR expression in blood was assessed using flow cytometry analysis of between 20 µl and 100 µl blood obtained from the tail vein at weekly intervals. Humane endpoints were agreed on with the ethics committee and were defined as >15% weight loss from starting weight, signs of hind leg paralysis or failing of the cage lid test. At the end of the experiment, spleens and bone marrow were collected. Briefly, spleens were processed by slicing the organ into chunks and passing through a 100 µm cell strainer (BD) before incubation with ACK lysing buffer (Gibco) for a maximum of 5 minutes. Splenocytes were then resuspended in PBS, 2% FCS before FACS analysis. Bone marrow was prepared by removing both epiphyses from the femur so that marrow could be flushed from the medullary cavity using RPMI-1640. Bone marrow cells were passed through a 100 µm cell strainer (BD) before incubation with ACK lysing buffer (Gibco) for a maximum of 5 minutes followed by resuspension in PBS, 2% FCS.

Acknowledgements We acknowledge the European Union's Horizon Europe research and innovation council for funding this work under the EIC Pathfinder Open NanoEngine project (grant 101098944). We also acknowledge partial support from the ProEVLifeCycle project (Horizon 2020, Marie Skłodowska-Curie grant agreement No 860303) for experiments performed by Pol Escudé Martínez de Castilla (University Medical Center Utrecht) and Martin van Royen (Erasmus University Medical Center). We thank Dr. Jelle Penders (Sparta) for assistance with experiments and data analysis and Dr. Michael Kalos for his critical review of the manuscript. Special thanks to Arnold Koekman and Simone Smits (University Medical Center Utrecht) for their contributions to experimental work, and to the staff of the Gemeenschappelijk Dierenlaboratorium in Utrecht for their support with animal studies. We also acknowledge TransCure Bioservices for conducting the in vivo study presented in Figure 4.

Contributors Conceptualization: MG, RS, JL. Methodology: JFB, EvD, DM, AA, ME, SN, DPV, HR, CZ, NS, ZL, PM. Investigation: JFB., EvD, DM, AA, ME, SN, DPV, HR, CZ. Writing and drafting: JFB, EvD, DM. Review and editing: JFB, EvD, DM, AA, ME, SN, DPV, MG, RS, JL. Guarantor: JL. AI language models were used to correct the language only.

Competing interests All authors are either full-time or part-time employees of NanoCell Therapeutics and hold equity or stock options in the company. MG, JL, EvD, DM, AA, ME, SN, NS and ZL are authors on patent applications related to this work. PM and MG are founders of Supercoiled GeneTx GmbH, which owns intellectual property rights to the minicircle DNA technology used in this study.

Patient consent for publication Not applicable.

Ethics approval Not applicable.

Provenance and peer review Not commissioned; externally peer reviewed.

Data availability statement Data are available upon reasonable request.

ORCID iDs
Jaime Fernández Bimbo http://orcid.org/0009-0002-4180-3507
Raymond Schiffelers http://orcid.org/0000-0002-1012-9815
Jacek Lubelski http://orcid.org/0009-0008-3148-2643

REFERENCES

1 Sengsayadeth S, Savani BN, Oluwole O, *et al*. Overview of approved CAR-T therapies, ongoing clinical trials, and its impact on clinical practice. *EJHaem* 2022;3:6–10.
2 Lu J, Jiang G. The journey of CAR-T therapy in hematological malignancies. *Mol Cancer* 2022;21:194.
3 Vormittag P, Gunn R, Ghorashian S, *et al*. A guide to manufacturing CAR T cell therapies. *Curr Opin Biotechnol* 2018;53:164–81: .
4 Mikhael J, Fowler J, Shah N. Chimeric Antigen Receptor T-Cell Therapies: Barriers and Solutions to Access. *JCO Oncol Pract* 2022;18:800–7.
5 Ahmed N, Sun F, Teigland C, *et al*. Chimeric Antigen Receptor T-Cell Access in Patients with Relapsed/Refractory Large B-Cell Lymphoma: Association of Access with Social Determinants of Health and Travel Time to Treatment Centers. *Transplantation and Cellular Therapy* 2024;30:714–25.
6 Bailey SR, Berger TR, Graham C, *et al*. Four challenges to CAR T cells breaking the glass ceiling. *Eur J Immunol* 2023;53:e2250039.
7 Tully S, Feng Z, Grindrod K, *et al*. Impact of Increasing Wait Times on Overall Mortality of Chimeric Antigen Receptor T-Cell Therapy in Large B-Cell Lymphoma: A Discrete Event Simulation Model. *JCO Clin Cancer Inform* 2019;3:1–9.
8 Chen AJ, Zhang J, Agarwal A, *et al*. Value of Reducing Wait Times for Chimeric Antigen Receptor T-Cell Treatment: Evidence From Randomized Controlled Trial Data on Tisagenlecleucel for Diffuse Large B-Cell Lymphoma. *Value Health* 2022;25:1344–51.
9 Bechman N, Maher J. Lymphodepletion strategies to potentiate adoptive T-cell immunotherapy - what are we doing; where are we going? *Expert Opin Biol Ther* 2021;21:627–37.
10 Michels A, Ho N, Buchholz CJ. Precision medicine: In vivo CAR therapy as a showcase for receptor-targeted vector platforms. *Mol Ther* 2022;30:2401–15.
11 Frank AM, Braun AH, Scheib L, *et al*. Combining T-cell-specific activation and in vivo gene delivery through CD3-targeted lentiviral vectors. *Blood Adv* 2020;4:5702–15.
12 Nicolai CJ, Parker MH, Qin J, *et al*. In vivo CAR T-cell generation in nonhuman primates using lentiviral vectors displaying a multidomain fusion ligand. *Blood* 2024;144:977–87.
13 Michels KR, Sheih A, Hernandez SA, *et al*. Preclinical proof of concept for VivoVec, a lentiviral-based platform for in vivo CAR T-cell engineering. *J Immunother Cancer* 2023;11:e006292.
14 Labbé RP, Vessillier S, Rafiq QA. Lentiviral Vectors for T Cell Engineering: Clinical Applications, Bioprocessing and Future Perspectives. *Viruses* 2021;13:1528.
15 Bouziana S, Bouzianas D. The Current Landscape of Secondary Malignancies after CAR T-Cell Therapies: How Could Malignancies Be Prevented? *IJMS* 2024;25:9518.

16 Annoni A, Gregori S, Naldini L, *et al*. Modulation of immune responses in lentiviral vector-mediated gene transfer. *Cell Immunol* 2019;342:103802.
17 Cordes N, Kolbe C, Lock D, *et al*. Anti-CD19 CARs displayed at the surface of lentiviral vector particles promote transduction of target-expressing cells. *Mol Ther Methods Clin Dev* 2021;21:42–53.
18 Wang C, Pan C, Yong H, *et al*. Emerging non-viral vectors for gene delivery. *J Nanobiotechnology* 2023;21:272.
19 Samaridou E, Heyes J, Lutwyche P. Lipid nanoparticles for nucleic acid delivery: Current perspectives. *Adv Drug Deliv Rev* 2020;154–155:37–63.
20 Rurik JG, Tombácz I, Yadegari A, *et al*. CAR T cells produced in vivo to treat cardiac injury. *Science* 2022;375:91–6.
21 Billingsley MM, Gong N, Mukalel AJ, *et al*. In Vivo mRNA CAR T Cell Engineering via Targeted Ionizable Lipid Nanoparticles with Extrahepatic Tropism. *Small* 2024;20:e2304378.
22 Kheirolomoom A, Kare AJ, Ingham ES, *et al*. In situ T-cell transfection by anti-CD3-conjugated lipid nanoparticles leads to T-cell activation, migration, and phenotypic shift. *Biomaterials* 2022;281.
23 Tombácz I, Laczkó D, Shahnawaz H, *et al*. Highly efficient CD4+ T cell targeting and genetic recombination using engineered CD4+ cell-homing mRNA-LNPs. *Mol Ther* 2021;29:3293–304.
24 Porter DL, Hwang W-T, Frey NV, *et al*. Chimeric antigen receptor T cells persist and induce sustained remissions in relapsed refractory chronic lymphocytic leukemia. *Sci Transl Med* 2015;7:303ra139:303–139:.
25 Shiqi L, Jiasi Z, Lvzhe C, *et al*. Durable remission related to CAR-T persistence in R/R B-ALL and long-term persistence potential of prime CAR-T. *Mol Ther Oncolytics* 2023;29:107–17.
26 Mayrhofer P, Schleef M, Jechlinger W. Use of minicircle plasmids for gene therapy. *Methods Mol Biol* 2009;542:87–104.
27 Smith TT, Stephan SB, Moffett HF, *et al*. In situ programming of leukaemia-specific T cells using synthetic DNA nanocarriers. *Nat Nanotechnol* 2017;12:813–20.
28 Schallon A, Synatschke CV, Jérôme V, *et al*. Nanoparticulate nonviral agent for the effective delivery of pDNA and siRNA to differentiated cells and primary human T lymphocytes. *Biomacromolecules* 2012;13:3463–74.
29 Riedl SAB, Kaiser P, Raup A, *et al*. Non-Viral Transfection of Human T Lymphocytes. *Processes (Basel)* 2018;6:188.
30 Suzuki H, Zelphati O, Hildebrand G, *et al*. CD4 and CD7 molecules as targets for drug delivery from antibody bearing liposomes. *Exp Cell Res* 1991;193:112–9.
31 Mayer KE, Mall S, Yusufi N, *et al*. T-cell functionality testing is highly relevant to developing novel immuno-tracers monitoring T cells in the context of immunotherapies and revealed CD7 as an attractive target. *Theranostics* 2018;8:6070–87.
32 Swart LE, Koekman CA, Seinen CW, *et al*. A robust post-insertion method for the preparation of targeted siRNA LNPs. *Int J Pharm* 2022;620:121741.
33 Kong R, Liu B, Wang H, *et al*. CAR-NK cell therapy: latest updates from the 2024 ASH annual meeting. *J Hematol Oncol* 2025;18:22:22:.
34 Gilleron J, Querbes W, Zeigerer A, *et al*. Image-based analysis of lipid nanoparticle-mediated siRNA delivery, intracellular trafficking and endosomal escape. *Nat Biotechnol* 2013;31:638–46.
35 Chen C, Chen C, Li Y, *et al*. Characterization of lipid-based nanomedicines at the single-particle level. *Fundam Res* 2023;3:488–504.
36 Hartjes TA, Slotman JA, Vredenbregt MS, *et al*. EVQuant; high-throughput quantification and characterization of extracellular vesicle (sub)populations. *Bioengineering* [Preprint] 2020.
37 Penders J, Pence IJ, Horgan CC, *et al*. Single Particle Automated Raman Trapping Analysis. *Nat Commun* 2018;9:4256.
38 Tao Z, Chyra Z, Kotulová J, *et al*. Impact of T cell characteristics on CAR-T cell therapy in hematological malignancies. *Blood Cancer J* 2024;14:213:213:.
39 Coughlan KA, Eybye M, Henderson N, *et al*. Improved therapeutic efficacy in two mouse models of methylmalonic acidemia (MMA) using a second-generation mRNA therapy. *Mol Genet Metab* 2024;143:108560.
40 Mullard A. In vivo CAR T cells move into clinical trials. *Nat Rev Drug Discov* 2024;23:727–30.
41 McCarron A, Donnelley M, McIntyre C, *et al*. Challenges of up-scaling lentivirus production and processing. *J Biotechnol* 2016;240:23–30.
42 Gogol-Döring A, Ammar I, Gupta S, *et al*. Genome-wide Profiling Reveals Remarkable Parallels Between Insertion Site Selection Properties of the MLV Retrovirus and the piggyBac Transposon in Primary Human CD4(+) T Cells. *Mol Ther* 2016;24:592–606.
43 Mayrhofer P, Jug H, Štrancar A, *et al*. Coordinating the in vivo processes for minicircle production - a novel approach to large scale manufacturing. *Bioengineering* [Preprint] 2018.
44 Doench JG, Fusi N, Sullender M, *et al*. Optimized sgRNA design to maximize activity and minimize off-target effects of CRISPR-Cas9. *Nat Biotechnol* 2016;34:184–91.